



Research article

Bogdanov-Takens bifurcation of a two species chemical reaction system and its stability using parameter identification

Xue Zhang, Jinzhao Wang, Feng Li, Hongwei Li* and Muhammad Marwan*

School of Mathematics and Statistics, Linyi University, Linyi 276005, Shandong, China

* **Correspondence:** Email: lihongwei@lyu.edu.cn, marwan78642@zjnu.edu.cn.

Abstract: In this paper, we mathematically analyzed a chemical reaction-based dynamical model to investigate codimension-two and codimension-three Bogdanov–Takens (BT) bifurcations and their impact on system dynamics. Generalized eigenvectors were first computed using normalization techniques to derive unfolding parameters for codim-two BT bifurcation. A codim-three BT bifurcation case was then obtained, with its unfolding parameters determined with the aid of the seven-step method. A control technique based on anonymous parameters and updated law was used to control oscillations in our considered dynamical system. Analytical results were validated through numerical simulations, highlighting the role of autocatalytic reactions $2D_1 \xrightarrow{\alpha_4} D_2$ and $2D_1 + D_2 \xrightarrow{\alpha_5} 3D_1$ in system behavior. These bifurcations generated oscillations, bi-stability, and excitability, behaviors essential for understanding and controlling complex chemical and biological systems.

Keywords: chemical reaction system; codim-two BT bifurcation; codim-three BT bifurcation; normalization; stability; updated law

1. Introduction

Chemistry, a field depending on chemical reactions, has a direct link with mathematics, especially while performing the balancing of chemical reactions before implementation in a laboratory. The dynamical and stability analysis of chemical reactions has attracted the attention of several researchers. A dynamical system designed from the chemical reaction of dioxide-iodine-malonic acid was studied by Din et al., [1] to identify Neimark-Sacker bifurcation and its control. In 2024 [2], the existence of Hopf bifurcation and its stability in an enzyme-catalyzed was discussed in the absence of spatial diffusions. Khan and Din [3] considered a fractional order autocatalator chemical reaction system for bifurcation analysis. The dynamics of fractional order Lorenz-based chemical chaotic system with its stability is discussed in [4]. Moreover, the higher codimension bifurcation of a modified Brusselator system in connection with strong resonances was part of a discussion in [5].

Although there are dynamical systems designed using chemical reactions, such as those by Huang et al., [6, 7], the enzyme-catalyzed reactions in [8], auto-catalytic glycolysis in [9], those by Belousov-Zhabotinsky [10], a chemical reaction system with single nonlinearity in [11], and the oregonator [12], and much more, two-species chemical reaction systems have shown a significance role in ecological and bio-chemical models. These models are used as a tool for providing a foundation in the advancement of medicines, environmental managements, and for the interactions between components, such as gene regulation and protein-protein. In the field of chemical engineering, two-species reaction systems play a role as an optimizer during a chemical reaction to achieve a desired product with minimum waste.

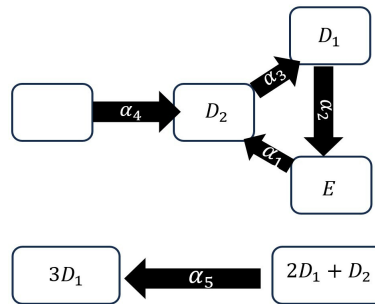


Figure 1. Schematic view of a two-species dynamical system.

A two dimensional autonomous dynamical system of kinetic differential equations [13] was designed using the schematic diagram given in Figure 1 and the chemical reactions $E \xrightarrow{\alpha_1} D_2$, $D_1 \xrightarrow{\alpha_2} E$, $D_2 \xrightarrow{\alpha_3} D_1$, $2D_1 \xrightarrow{\alpha_4} D_2$, $2D_1 + D_2 \xrightarrow{\alpha_5} 3D_1$

$$\begin{cases} \frac{d\tilde{x}}{d\tilde{t}} = -\alpha_2\tilde{x} - 2\alpha_4\tilde{x}^2 + \alpha_3\tilde{y} + \alpha_5\tilde{x}^2\tilde{y}, \\ \frac{d\tilde{y}}{d\tilde{t}} = \alpha_1 + \alpha_4\tilde{x}^2 - \alpha_3\tilde{y} - \alpha_5\tilde{x}^2\tilde{y}. \end{cases} \quad (1.1)$$

The system describes two species, D_1 (represented by \tilde{x}) and D_2 (represented by \tilde{y}), interacting through a set of chemical reactions: $E \xrightarrow{\alpha_1} D_2$, the environment E produces D_2 at rate α_1 . In $D_1 \xrightarrow{\alpha_2} E$, D_1 degrades back to the environment at rate α_2 , and in $D_2 \xrightarrow{\alpha_3} D_1$, D_2 is converted into D_1 at rate α_3 . $2D_1 \xrightarrow{\alpha_4} D_2$ shows the two D_1 molecules combining to form D_2 at rate α_4 , whereas in $2D_1 + D_2 \xrightarrow{\alpha_5} 3D_1$, a tri-molecular reaction occurs, where D_2 catalyzes the production of D_1 at the rate of α_5 . The number of free parameters is further reduced in system (1.1) by transforming into the non-dimensional form Eq (1.2). This transformation process is obtained through the rescaling of time, state variables, and involved parameters. Suppose the original dimensional variables are denoted by \tilde{x} and \tilde{y} (having units of concentration), and time by \tilde{t} . The chemical reactions and their rate constants $\alpha_i > 0$ are given in the schematic diagram (Figure 1). We introduce dimensionless variables:

$$x = \frac{\tilde{x}}{K}, \quad y = \frac{\tilde{y}}{K}, \quad t = \alpha_3\tilde{t},$$

where K is a reference concentration scale. Selecting $K \approx \sqrt{\frac{\alpha_3}{\alpha_5}}$, then system (1.1) reduces to the

dimensionless form:

$$\begin{cases} \frac{dx}{dt} = -ax - 2x^2 + by + x^2y, \\ \frac{dy}{dt} = c + x^2 - by - x^2y. \end{cases} \quad (1.2)$$

The detailed relationship between the original rate constants α_i and the dimensionless parameters a , b , c are given in Table 1.

Table 1. The transformations of dimensional rate constants into dimensionless parameters.

Dimensionless	Transformation	Physical interpretation
a	$\frac{\alpha_2}{\alpha_3}$	Ratio of degradation to conversion rate
b	$\frac{\alpha_1}{\alpha_3 K}$	Environmental production rate of D_2 ($E \rightarrow D_2$)
c	$\frac{\alpha_4 K}{\alpha_3}$	Auto-catalytic dimerization rate ($2D_1 \rightarrow D_2$)
	$K = \sqrt{\frac{\alpha_3}{\alpha_5}}$	Elimination of α_5

System (1.2) has been considered by several researchers for various purposes in the literature. In 2000, Erle [14] proved that stable closed orbits in a two species model does not exist with a condition if there are no additional reaction steps beyond the number of reactants. Azimi et al., [15] investigated the multi-stability and limit cycles using the numerical approach in system (1.2). The necessary and sufficient conditions, using symbolic computation to determine limit cycle bifurcates from a stationary point, are given in [16], whereas two nested limit cycles of the two species model is illustrated by Nagy et al., [17]. In 2023, the considered kinematic chemical reaction system gained importance as part of discussions in chemical reaction networks [18] and was shown to exhibit Hopf bifurcation with at least three species and four irreversible reactions, respectively. Din and Saeed [13] in 2023 discussed the existence of Hopf bifurcation and stabilized it with the aid of a control method.

The changing topological structure of a given dynamical system with the changes in the involved parameters is called bifurcation, and the parameter due to which such types of changes occur is known as the bifurcation parameter. Bifurcation theory is not only limited to mathematical purposes but has potential applications in other fields [19–22]. Although there are several types of bifurcations, the categorization with codim has made it more feasible in bifurcation theory. Higher codim bifurcations include cusp [23] and bautin [24], but the BT bifurcation has received the most attention from researchers for its enriched dynamics around the bifurcation point.

The condition of satisfying zero eigenvalues with multiplicity two is the leading step toward the existence of codim-two bifurcation cases. Among the above-mentioned codim-two bifurcations, several researchers have studied BT and derived analytical formulas for its practical computations. In 2005, Kuznetsov [25] used the center manifold theorem and derived analytical formulas for the computation of normal forms of codim-two and codim-three BT bifurcations. While the work is essential and easy to use for achieving normal forms, the way of finding unfolding parameters was not discussed. In 2010, Carrlio et al., [26] provided a technique to calculate the unfolding parameter for BT bifurcation but with the limitation that the study was confined to codim-two only, which Liu and Liu [27] used in the computation of BT bifurcation on the Hindmarsh-Rose model. Similarly, Peng and Jiang [28] derived analytical formulas for the practical computation of BT bifurcation but with the same limitation. A

developed technique, namely the seven-step rule [29, 30], has been important in the computation of normal forms and unfolding parameters.

However, the BT bifurcation has a great record in the literature, starting from the work of Takens [31] and Bogdanov [32] in 1974~1981. In 2016, Liu et al., [33] investigated a predator-prey model for the possibility of BT bifurcation using normal form theory. The different topological cases of BT bifurcation are discussed by Lu et al., [34]. In 2022, Wang and Yu [35] proposed a novel predator-prey model and derived several parametric conditions to explore codim-two and codim-three bifurcations. The application of this bifurcation is not limited to specific models but is found in a variety of potential applications [36–38].

The existence of bifurcations, while beneficial, can be problematic in sensitive real-life models such as chemical reactions, building structures, and aerodynamics. Therefore, control in such systems, particularly for bifurcation parameters, is essential. There are several control techniques in the literature such as robust and optimization [39], event-triggered [40], hybrid [41], active and passive [42], and sliding-mode [43] techniques.

To the best of our knowledge, no researcher has investigated the physical impact of higher codimension bifurcations, particularly BT bifurcation, on the two-species chemical reaction system (1.2), nor has implemented any control strategy to regulate bifurcation at specific parameters. The BT bifurcation is significant in chemical systems as it governs transitions between stable steady states, oscillatory, and excitable dynamics. In this paper, we address the gap by analyzing codim-two and codim-three BT bifurcations in system (1.2) using practical computation and the seven-step rule, respectively.

The remainder of the paper is organized as follows: In Section 2, we provide the computation and discussion of codimension two and three Bogdanov-Takens bifurcations. In Section 3, the two bifurcation parameters are considered anonymous, and we use Lyapunov theory to discuss the stability in the two species-based chemical reaction system. The paper is concluded in Section 4.

2. BT bifurcation analysis in a two species chemical reaction system

In this section, the dynamics of chemical system (1.2) is further enhanced with the study of codim-two and three Bogdanov-Takens bifurcations. The analytical technique [26, 27] for codim-two case is utilized, while codim-three bifurcation is obtained with their unfolding parameters using the seven-step rule [30].

Theorem 2.1. *System (1.2) undergoes a codim-2 BT bifurcation for the reaction rates $b = \frac{1}{4}(4a - a^2)$, $c = -\frac{a^2}{4}$ with $a_2b_2 \neq 0$.*

Proof. Consider the semi-trivial equilibria $E_+(x_*, y_*)$ of system (1.2), so that the Jacobian matrix at E_+ is

$$J(E_+) = \begin{pmatrix} -a + 2x_*y_* - 4x_* & b + x_*^2 \\ -2x_*(y_* - 1) & -b - x_*^2 \end{pmatrix}. \quad (2.1)$$

A two dimensional system exhibits double zero eigenvalues by solving the trace and determinant of the Jacobian matrix (2.1) at the corresponding equilibrium point equaling zero, simultaneously. Further,

the equilibria E_+ can be computed by solving

$$\begin{cases} -ax_* - 2x_*^2 + by_* + x_*^2y_* = 0, \\ c + x_*^2 - by_* - x_*^2y_* = 0. \end{cases} \quad (2.2)$$

The trace and determinant of the matrix are $\text{Tr}J(E_+) = -a - b - x_*^2 + 2x_*y_* - 4x_*$ and $\text{Det}J(E_+) = (a + 2x_*)(b + x_*^2)$. Solving $\text{Tr} J(E_+) = \text{Det} J(E_+) = 0$, along with Eq (2.2) to get $b = b_* = \frac{1}{4}(4a - a^2)$ and $c = c_* = -\frac{a^2}{4}$ as the BT bifurcation parameters. Moreover, substituting b_* and c_* into Eq (2.2), the equilibrium point of system (1.2) becomes $E(-\frac{a}{2}, 0)$, at which the Jacobian matrix of the system is

$$J(E) = \begin{pmatrix} a & a \\ -a & -a \end{pmatrix}. \quad (2.3)$$

Both eigenvalues of the matrix (2.3) are zero. Therefore, there are four real linearly independent (generalized) eigenvectors, $p_{0,1} \in \mathbb{R}^n$, $q_{0,1} \in \mathbb{R}^n$, such that $Jq_0 = 0$, $Jq_1 = q_0$ and $J^T p_1 = 0$, $J^T p_0 = p_1$. Solving these relations for the vectors, we get the following left and right generalized vectors:

$$q_0 = \begin{pmatrix} 1 \\ -1 \end{pmatrix}, \quad q_1 = \begin{pmatrix} \frac{1}{a} \\ 0 \end{pmatrix}, \quad p_0 = \begin{pmatrix} 0 \\ -1 \end{pmatrix}, \quad p_1 = \begin{pmatrix} a \\ a \end{pmatrix}$$

that satisfy the orthogonality conditions $\langle p_0, q_0 \rangle = \langle p_1, q_1 \rangle = 1$ and $\langle p_0, q_1 \rangle = \langle p_1, q_0 \rangle = 0$. The inner product $\langle \cdot, \cdot \rangle$ is defined as the standard Euclidean inner product in \mathbb{R}^2 . Further, we rewrite system (1.2) as $\frac{dX}{dt} = F(X, \mu)^*$, where $X = (x, y)^T$, $\mu = (a, b, c)^T$ and

$$F(X, \mu) = \begin{pmatrix} -ax - 2x^2 + by + x^2y \\ c + x^2 - by - x^2y \end{pmatrix}.$$

The complete BT bifurcation set of system (1.1) is

$$BT = \{(X_0, \mu_0) | X_0 = (-\frac{a}{2}, 0), \mu_0 = (a, b_*, c_*)\}. \quad (2.4)$$

According to the formulas given in Appendix A for \bar{a} , \bar{b} , we get

$$\bar{a} = a_2 = -a, \quad \bar{b} = b_2 = 2a - 4. \quad (2.5)$$

To avoid confusion, we use a_2 and b_2 as the parameters of the normal form. Now, using the theorem in [26], we have that system (1.2) is locally topologically equivalent to

$$\begin{cases} \frac{d\zeta_1}{dt} = \zeta_2, \\ \frac{d\zeta_2}{dt} = \beta_1 + \beta_2\zeta_1 + a_2\zeta_1^2 + b_2\zeta_1\zeta_2. \end{cases} \quad (2.6)$$

System (2.6) is the normal form for the codim-2 BT bifurcation truncated at quadratic order. Higher-order terms are eliminated through smooth, near-identity transformations and do not affect the local

*The formulas from [26] used in this analysis depends on $F(X, \mu)$. This vector field must be sufficiently smooth (at least C^4) in a neighborhood of (X_0, μ_0) . Moreover, the non-degeneracy condition $\bar{a}\bar{b} \neq 0$ must hold, and the map from the original parameters to the unfolding parameters should satisfy the regularity condition; i.e., the Jacobian matrix should be non-singular at $\mu=\mu_0$.

topological equivalence, as guaranteed by the Center Manifold Theorem. If we choose $\lambda_1 = b - b_*$ and $\lambda_2 = c - c_*$ as bifurcation parameters, then

$$\lambda_1 = b - \frac{1}{4}(4a - a^2), \quad \lambda_2 = c + \frac{a^2}{4}$$

The following unfolding parameters are obtained using the formulas given in Appendix A

$$\beta_1 = a\lambda_2, \quad \beta_2 = -\frac{a(\lambda_1 + \lambda_2)}{a - 2}.$$

Now, using the change of variables by

$$\zeta_1 = \left(\frac{-a}{(2a - 4)^2}\right)\eta_1, \quad \zeta_2 = \left(\frac{-a^2}{(2a - 4)^3}\right)\eta_2, \quad t = \left(\frac{2a - 4}{a}\right)t_1$$

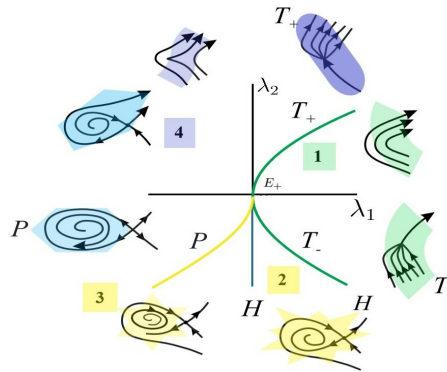


Figure 2. Generic local curves of the system (2.7) around BT bifurcation point [25].

We obtain

$$\begin{cases} \frac{d\eta_1}{dt_1} = \eta_2, \\ \frac{d\eta_2}{dt_1} = \mu_1 + \mu_2\eta_1 + \eta_1^2 - \eta_1\eta_2, \end{cases} \tag{2.7}$$

where

$$\mu_1 = -\frac{16\lambda_2(a - 2)^4}{a^2}, \quad \mu_2 = -\frac{4(a - 2)(\lambda_1 + \lambda_2)}{a}.$$

Moreover, under the conditions of Theorem 2.1, system (1.2) undergoes a Bogdanov-Takens bifurcation of codim-two if and only if $a \neq 2$. Let $b = \frac{1}{4}(4a - a^2) + \lambda_1$, $c = -\frac{a^2}{4} + \lambda_2$, and $a \neq 2$, then system (1.2) is locally topologically equivalent to

$$\begin{cases} \frac{d\eta_1}{dt_1} = \eta_2, \\ \frac{d\eta_2}{dt_1} = -\frac{16\lambda_2(a-2)^4}{a^2} - \frac{4(a-2)(\lambda_1+\lambda_2)}{a}\eta_1 + \eta_1^2 - \eta_1\eta_2, \end{cases} \tag{2.8}$$

which has the following local representations of the bifurcation curves in a small neighborhood around the semi-trivial equilibria E_+

(1) Saddle-node bifurcation curve:

$$SN = \{(\lambda_1, \lambda_2) | \lambda_2 = 8a - \lambda_1 + (4 - 2a)\sqrt{a^2 - 4a + \lambda_1 + 4} - 2a^2 - 8\}.$$

(2) Hopf bifurcation curve:

$$H = \{(\lambda_1, \lambda_2) | -\frac{16\lambda_2(a-2)^4}{a^2} = 0, \frac{(a-2)(\lambda_1 + \lambda_2)}{a} > 0\}.$$

(3) Homoclinic bifurcation curve:

$$HL = \{(\lambda_1, \lambda_2) | \lambda_2 = \sigma_2 - \lambda_1 - \frac{25a}{3} + \frac{25a^2}{12} - \sigma_1 + \frac{25}{3} + o(|\lambda_1, \lambda_2|^2), \frac{(a-2)(\lambda_1 + \lambda_2)}{a} > 0\},$$

for $\sigma_1 = \frac{25a\sqrt{a^2-4a-\frac{24\lambda_1}{25}+4}}{12}$ and $\sigma_2 = \frac{25\sqrt{a^2-4a-\frac{24\lambda_1}{25}+4}}{6}$.

Figure 2 shows the local topological structure, characterized by the equilibria, the generation of limit cycles through Hopf bifurcation, and their disappearance with homoclinic loops, and is robust for parameter values that move the overall dynamics of the system into the positive quadrant. As the parameters (b, c) are varied away from (b_*, c_*), the relevant dynamics (such as a stable limit cycle or a region of bistability) can move into the positive quadrant, becoming observable in a chemically realistic regime.

The BT bifurcation diagram for the local bifurcation curves is given in Figure 2, where four regions can be observed. Starting from region 1, the BT bifurcation is associated with a saddle-node bifurcation, where two equilibrium points collide and annihilate each other. In this region, bi-stability shows that the trajectory remains even if the parameters are changed slightly until a critical point is reached, where it abruptly switches to the second regime. The trajectory then jumps into the second region where it satisfies the Hopf bifurcation condition. Finally, the trajectories of system (1.2) enter region P , where the BT bifurcation can lead to homoclinic orbits, and the trajectories spend more time near an unstable equilibrium before transitioning into a different state. This whole cycle from region 1 to region 4 creates a phenomenon of appearance and disappearance of the limit cycle.

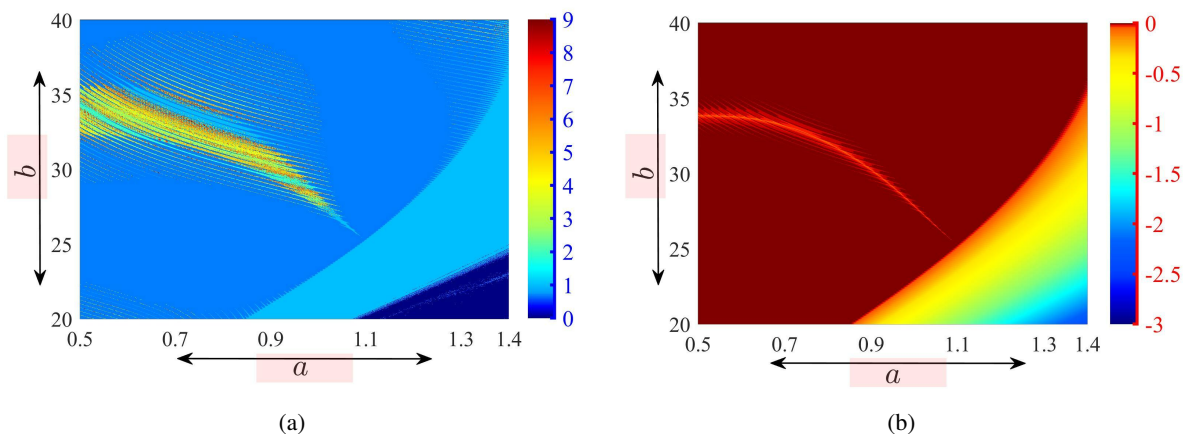


Figure 3. (a) Two-parametric bifurcation diagram and its (b) Lyapunov exponent determining the dynamics of system (1.2).

The multi-parameter bifurcation diagram and Lyapunov exponents [44] have a significant role in providing detailed information around the high codimension bifurcation point. In Figure 3(a), the BT bifurcation parameters are to generate its bifurcation diagram, where the periodicity of bifurcation from lower to higher is shown in the range of [1,9]. Figure 3(b) is the highest Lyapunov exponent for parameters b and c in our considered chemical model, completely covering the dynamics shown in its bifurcation diagram.

2.1. Chemical feasibility and biological interpretation of the bifurcation point

The BT bifurcation point (X_0, μ_0) identified in Theorem 2.1 is at the equilibrium $E\left(-\frac{a}{2}, 0\right)$. For the model to be chemically meaningful, the concentrations must satisfy $x \geq 0$ and $y \geq 0$. The x -coordinate of this point imposes the condition $a \leq 0$. Given that the original model parameters α_i are positive, the non-dimensional parameter a is also positive, implying $-\frac{a}{2} < 0$. Therefore, the BT point E lies outside the chemically feasible positive quadrant for the nominal parameter range of interest. According to real conditions, the system exhibits codim-1 bifurcations, such as Hopf, but is not suitable for higher codimension bifurcations. Consequently, the bifurcation set $BT = \{(X_0, \mu_0)\}$ should be understood mathematically.

Physically, system (2.8) interprets, in the first region, the concentration rates; i.e., D_1 and D_2 remain constant, and the transition to a state oscillate or diverge as a result. This collapse of steady states can disrupt the balance of chemical reaction pathways, leading to unpredictable behavior in the production and consumption of D_1 and D_2 . In region 1, the BT bifurcation can lead to bistability, where the system has two stable steady states for the same set of parameters and the reaction pathways can settle into two distinct regimes with the higher concentration of D_1 and lower concentration of D_2 in first regime and vice versa in the second regime. Entering the second region, the concentrations of D_1 and D_2 begin to oscillate. This situation occurs due to the presence of pure imaginary eigenvalues exhibiting Hopf bifurcation. Moreover, the conversion rate of D_1 to E (α_2) and D_2 to D_1 (α_3) vary periodically. The autocatalytic steps $2D_1 \xrightarrow{\alpha_4} D_2$ and $2D_1 + D_2 \xrightarrow{\alpha_5} 3D_1$ also exhibit periodic behavior, leading to fluctuations in the production and consumption of D_1 and D_2 . Consequently, small perturbations in the concentrations of D_2 could lead to a sudden spike in D_1 production due to the autocatalytic reaction $2D_1 + D_2 \xrightarrow{\alpha_5} 3D_1$ and vice versa.

Theorem 2.2. Consider $a = 2$ in Eq (2.5), then system (1.2) undergoes the codim-3 BT bifurcation.

Proof. In Theorem 2.1, b and c are computed as bifurcation parameters for the calculation of codim-2 BT bifurcation, whereas $a = 2$ results in the $a_2 b_2 = 0$, which shows the possibility of codim-3 BT bifurcation. Hence, starting with the substitutions of, $a = 2 + r_1$, $b = \frac{1}{4}(4a - a^2) + r_2$, and $c = -\frac{a^2}{4} + r_3$ into system (1.2), where r_1 , r_2 , and r_3 are arbitrarily small parameters. However, there are several practical computation methods designed so far but the seven-step method has shown much importance among all. For this, we translate the equilibrium point $(-1, 0)$ to the origin $(0, 0)$, and system (1.2) becomes

$$\begin{aligned} \frac{dx}{dt} &= r_1 + 2x - r_1 x - 2x^2 + 2y + r_2 y - 2xy + x^2 y, \\ \frac{dy}{dt} &= r_3 - 2x + x^2 - 2y - r_2 y + 2xy - x^2 y. \end{aligned} \quad (2.9)$$

Now, with the aid of the seven-step method, the following calculations are obtained: In each step R_1, R_2, \dots, R_6 obeys the property given in Eq (2.17).

Step 1: Let $u = x$, $v = r_1 + 2x - r_1x - 2x^2 + 2y + r_2y - 2xy + x^2y$, and carry out a Taylor expansion at the origin to obtain

$$\begin{aligned}\frac{du}{dt} &= v, \\ \frac{dv}{dt} &= -r_1uv - 4r_1u + 2r_1 - r_2uv - r_2v - 2r_3u + 2r_3 - u^4 \\ &\quad - u^3v + 2u^3 + \frac{u^2v^2}{2} - 3u^2v - 2u^2 - v^2 + R_1(u, v, r).\end{aligned}\tag{2.10}$$

Step 2: Set $u = \frac{1}{2}\Upsilon_1x^2 + x$, $v = \Upsilon_1xy + y$, a near identity transformation for (u, v) near the origin, for the elimination of v^2 in Eq (2.10). A Taylor expansion of the system is performed with $\Upsilon_1 = -1$ and considers only the first few terms to transform system (2.10) as

$$\begin{aligned}\frac{dx}{dt} &= y, \\ \frac{dy}{dt} &= -r_1xy - 2r_1x + 2r_1 - r_2xy - r_2y + 2r_3 - \frac{5x^4}{2} \\ &\quad + 2x^3y + 2x^3 - 3x^2y - 2x^2 + 2xy^2 + R_2(x, y, r).\end{aligned}\tag{2.11}$$

Step 3: We let $x = \frac{1}{6}\Upsilon_2u^3 + \frac{1}{2}\Upsilon_3u^2v + u$, $y = \frac{1}{2}\Upsilon_2u^2v + \Upsilon_3uv^2 + v$ to remove xy^2 and y^3 , where Υ_2 and Υ_3 are the coefficients of eliminating terms, respectively. We get $\Upsilon_2 = 2$ and $\Upsilon_3 = 0$ after some calculations, and system (2.11) is transformed into

$$\begin{aligned}\frac{du}{dt} &= v, \\ \frac{dv}{dt} &= -r_1uv - 2r_1u + 2r_1 - r_2uv - r_2v + 2r_3 + 2u^3v + 2u^3 - 3u^2v - 2u^2 + R_3(u, v, r).\end{aligned}\tag{2.12}$$

Step 4: In this step, we eliminate u^3 in system (2.12) by considering the transformation set $u = x^3(\frac{3\Theta_2}{16\Theta_1^2} - \frac{\Theta_3}{5\Theta_1}) - \frac{\Theta_2}{4\Theta_1}x^2 + x$, $v = y$, where Θ_1 , Θ_2 and Θ_3 are the coefficients of u^2 , u^3 , and u^4 . System (2.12) is transformed in the following form with $\Theta_1 = -2$, $\Theta_2 = 2$ and $\Theta_3 = 0$

$$\begin{aligned}\frac{dx}{dt} &= y, \\ \frac{dy}{dt} &= -r_1xy - r_1x + 2r_1 - \frac{3r_2xy}{2} - r_2y + r_3x + 2r_3 - x^3y - 3x^2y - 2x^2 + R_4(x, y, r).\end{aligned}\tag{2.13}$$

Step 5: Considering $x = u$, $y = \frac{1}{36}\Theta^2v^3 + \frac{1}{3}\Theta v^2 + v$ to transform system (2.13) into the following form

$$\begin{aligned}\frac{du}{dt} &= v, \\ \frac{dv}{dt} &= \frac{r_1uv}{2} - r_1u - 3r_1v + 2r_1 - \frac{3r_2uv}{2} - r_2v - \frac{3r_3uv}{2} + r_3u - 3r_3v + 2r_3 - u^3v - 2u^2 + R_5(u, v, r),\end{aligned}\tag{2.14}$$

by eliminating x^2y . In particular, the coefficient ratio Θ is given by $\Theta = \frac{\Theta_4}{\Theta_5}$, where $\Theta_4 = -3$ and $\Theta_5 = -2$ are the coefficients of x^2y and x^2 .

Step 6: In this step, we make the following changes of variables $u = \Theta_6^{\frac{1}{5}}\Theta_7^{-\frac{2}{5}}x$ and $v = \Theta_6^{\frac{4}{5}}\Theta_7^{-\frac{3}{5}}y$, with the time re-parametrization $t = \Theta_6^{-\frac{3}{5}}\Theta_7^{\frac{1}{5}}\tau$, where Θ_6 and Θ_7 are the coefficients of u^2 and u^3v . System (2.14) becomes

$$\begin{aligned} \frac{dx}{d\tau} &= y, \\ \frac{dy}{d\tau} &= -\frac{r_1xy}{2 \times 2^{2/5}} - \frac{r_1x}{2 \times 2^{1/5}} - \frac{3r_1y}{2^{3/5}} - \frac{r_1}{2^{2/5}} + \frac{3r_2xy}{2 \times 2^{2/5}} - \frac{r_2y}{2^{3/5}} + \frac{3r_3xy}{2 \times 2^{2/5}} \\ &\quad + \frac{r_3x}{2 \times 2^{1/5}} - \frac{3r_3y}{2^{3/5}} - \frac{r_3}{2^{2/5}} + x^3y + x^2 + R_6(x, y, r) \end{aligned} \tag{2.15}$$

with $\Theta_6 = -2$ and $\Theta_7 = -1$, where $R_6(x, y, r)$ has the property (2.17).

Step 7: We let $x = u - \frac{\sigma_1}{2}$, $y = v$, and $\sigma_1 = -\frac{r_1-r_3}{2 \times 2^{1/5}}$ for the coefficient of x in system (2.15). The final transformation is

$$\begin{cases} \frac{du}{d\tau} = v, \\ \frac{dv}{d\tau} = \xi_1 + \xi_2v + \xi_3uv + u^2 + u^3v + R(u, v, r), \end{cases} \tag{2.16}$$

where

$$\xi_1 = -\frac{r_1 + r_3}{2^{2/5}}, \quad \xi_2 = -\frac{3r_1 + r_2 + 3r_3}{2^{3/5}}, \quad \xi_3 = -\frac{r_1 - 3r_2 - 3r_3}{2 \times 2^{2/5}},$$

and

$$R(u, v, r) = y^2O(|u, v|^2) + O(|u, v|^5) + O(r) \times (O(v^2) + O(|u, v|^3)) + O(r^2)O(|u, v|). \tag{2.17}$$

The final form given in system (2.16) is obtained after a sequence of near-identity transformations and is truncated to include terms up to cubic order, which is necessary to capture the dynamics of the codim-3 bifurcation. The determinant of the Jacobian matrix $\frac{D(\xi_1, \xi_2, \xi_3)}{D(r_1, r_2, r_3)} = \frac{1}{2^{2/5}}$ of system (2.16) for small r is non-zero. Therefore, local bifurcation curves are possible.

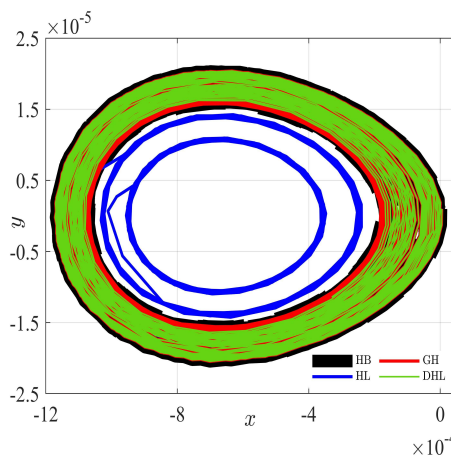


Figure 4. Phase portraits of local bifurcation curves in codim-3 BT bifurcation.

In Figure 4, limit cycles are plotted in which the black is obtained using the Hopf bifurcation (HB), the blue colored limit cycle is generated with the help of Homoclinic loop (HL) bifurcation, the generalized Hopf bifurcation (GH) can be seen in red, and the degenerate case of homoclinic bifurcation (DHL) curve surrounded within HB and GH is shown as green trajectories. Mathematically, all the possible local bifurcation curves are calculated using the analytical formulas for their corresponding critical surfaces given by Zeng et al., [30];

1. Saddle-node bifurcation occurs:

$$SN = \{(\xi_1, \xi_2, \xi_3) \mid \xi_1 = 0\}.$$

2. Hopf bifurcation at the critical surface:

$$HB = \{(\xi_1, \xi_2, \xi_3) \mid \xi_1 < 0, \xi_2 = (\xi_3 - \xi_1) \sqrt{-\xi_1}\}.$$

3. Homoclinic loop bifurcation occurs from the critical surface:

$$HL = \left\{(\xi_1, \xi_2, \xi_3) \mid \xi_1 < 0, \xi_2 = \frac{5}{7} \left(\xi_3 - \frac{179}{11} \xi_1\right) \sqrt{-\xi_1}\right\}.$$

4. Generalized Hopf bifurcation occurs for $\xi_1 < 0$ from the critical curve:

$$GH = \{(\xi_1, \xi_2, \xi_3) \mid \xi_2 = -4\xi_1 \sqrt{-\xi_1}, \xi_3 = -3\xi_1\}.$$

5. Degenerate homoclinic bifurcation occurs for $\xi_1 < 0$ from the critical curve:

$$DHL = \left\{(\xi_1, \xi_2, \xi_3) \mid \xi_2 = -\frac{70}{11} \xi_1 \sqrt{-\xi_1}, \xi_3 = \frac{81}{11} \xi_1\right\}.$$

6. Double limit cycle bifurcation occurs from a critical surface, which is tangent to the HB on the critical curve GH, and tangent to the HL on the critical curve DHL.

The condition $a_2 b_2 \neq 0$ (with $a_2 = -a$, $b_2 = 2a - 4$) and the subsequent nondegeneracy conditions for the codim-3 case ensure that this organizing center is not degenerate, and, thus, the predicted bifurcation scenarios are generic and can manifest in the feasible region for appropriate parameter choices. The numerical simulations in Figures 3 and 5, which show dynamics in the positive quadrant, serve as a validation of this principle.

Physically, the codimension-three BT bifurcation in the chemical system leads to several critical dynamical changes with significant chemical implications. The saddle-node bifurcation (SN) results in the sudden loss or creation of steady states, causing abrupt transitions in the concentrations of D_1 and D_2 , which can disrupt the balance of the autocatalytic reactions $2D_1 \xrightarrow{\alpha_4} D_2$ and $2D_1 + D_2 \xrightarrow{\alpha_5} 3D_1$. The HB introduces oscillatory dynamics, leading to periodic variations in species concentrations, which is crucial for systems requiring rhythmic behavior, such as chemical oscillators. The HL induces excitable dynamics, where small perturbations in D_1 or D_2 can trigger large-scale changes through the autocatalytic pathways, making the system highly sensitive to external influences. The GH further enriches the oscillatory behavior, potentially leading to multi-frequency patterns in the reaction

rates, including the autocatalytic steps. The DHL can result in chaotic dynamics, where the system becomes unpredictable and highly sensitive to parameter changes, particularly affecting the autocatalytic feedback loops. Finally, the double limit cycle bifurcation creates complex interactions between multiple oscillatory states, leading to intricate dynamical regimes that influence the autocatalytic production and consumption of D_1 and D_2 . Together, these bifurcations highlight the system's sensitivity to parameter variations and its potential for rich, complex behavior, which is critical for controlling and predicting the outcomes of the chemical reactions, especially those involving autocatalysis.

3. Stability of chemical reaction system (1.2)

In Section 2, we use analytical formulas to find the normal forms for finding the existence of higher codimension bifurcation in autocatalytic chemical reaction system (1.2). It has been observed that the parameters b and c play vital roles in determining BT bifurcation. However, a negligible oscillation during a chemical process can cause severe damage to the scientist, energy, and cost. Moreover, the control of such systems at the bifurcation parameters is necessary; therefore, in this section, we use Lyapunov theory to bring stability in system (1.2) with the assumption that the bifurcation parameters b and c are anonymous. For this purpose, we rewrite system (1.2) as

$$\begin{cases} \frac{dx}{dt} = -ax - 2x^2 + \hat{b}(t)y + x^2y + \rho_1(t), \\ \frac{dy}{dt} = \hat{c}(t) + x^2 - \hat{b}(t)y - x^2y + \rho_2(t), \end{cases} \quad (3.1)$$

where $\hat{b}(t)$ and $\hat{c}(t)$ are unknown time dependent parameters, and $\rho_1(t)$, $\rho_2(t)$ are control inputs that will be determined using the negative definiteness property of the considered Lyapunov function. We introduce and differentiate the error terms $e_1 = x - x_*$ and $e_2 = y - y_*$ to get the following error dynamical system:

$$\begin{cases} \frac{de_1}{dt} = -ae_1 - ax_* - 2(e_1^2 + 2e_1x_* + x_*^2) + \hat{b}e_2 + \hat{b}y_* \\ \quad + e_1^2e_2 + e_2x_*^2 + e_1^2y_* + x_*^2y_* + 2e_1e_2x_* + 2e_1x_*y_* + \rho_1(t), \\ \frac{de_2}{dt} = \hat{c} + e_1^2 + 2e_1x_* + x_*^2 - \hat{b}e_2 - \hat{b}y_* - e_1^2e_2 \\ \quad - e_2x_*^2 - e_1^2y_* - x_*^2y_* - 2e_1e_2x_* - 2e_1x_*y_* + \rho_2(t). \end{cases} \quad (3.2)$$

To find the suitable controller for system (3.2), we use the Lyapunov function

$$v_L = \frac{1}{2}(e_1^2 + e_2^2 + e_b^2 + e_c^2) \quad (3.3)$$

satisfying $v_L(0) > 0$ for all time t . Differentiating Eq (3.3), we get

$$\frac{dv_L}{dt} = e_1 \frac{de_1}{dt} + e_2 \frac{de_2}{dt} - e_b \frac{d\hat{b}}{dt} - e_c \frac{d\hat{c}}{dt}, \quad (3.4)$$

where $\frac{de_b}{dt} = -\frac{d\hat{b}}{dt}$ and $\frac{de_c}{dt} = -\frac{d\hat{c}}{dt}$. Substituting Eq (3.2) into Eq (3.4) with $e_b = b - \hat{b}(t)$ and $e_c = c - \hat{c}(t)$,

we get

$$\left\{ \begin{array}{l} \frac{dv_I}{dt} = -ae_1^2 - ax_*e_1 - 2(e_1^3 + 2e_1^2x_* + e_1x_*^2) + \hat{b}e_1e_2 \\ \quad + \hat{b}e_1y_* + e_1^3e_2 + e_1e_2x_*^2 + e_1^3y_* + e_1x_*^2y_* \\ \quad + 2e_1^2e_2x_* + 2e_1^2x_*y_* + \hat{c}e_2 + e_1^2e_2 \\ \quad + 2e_1e_2x_* + e_2x_*^2 - \hat{b}e_2^2 - \hat{b}e_2y_* - e_1^2e_2^2 \\ \quad - e_2^2x_*^2 - e_1^2e_2y_* - e_2x_*^2y_* - 2e_1e_2^2x_* \\ \quad - 2e_1e_2x_*y_* + e_1\rho_1(t) + e_2\rho_2(t) - e_b\frac{db}{dt} - e_c\frac{dc}{dt}. \end{array} \right. \quad (3.5)$$

In view of systems (3.2)–(3.5), the control inputs ρ_1 and ρ_2 are selected as

$$\left\{ \begin{array}{l} \rho_1(t) = -\kappa_1e_1 + ax_* + 2(e_1^2 + 2e_1x_* + x_*^2) - be_2 - by_* \\ \quad - e_1^2e_2 - e_2x_*^2 - e_1^2y_* - x_*^2y_* - 2e_1e_2x_* - 2e_1x_*y_*, \\ \rho_2(t) = -\kappa_2e_2 - c - e_1^2 - 2e_1x_* - x_*^2 + be_2 + by_* + e_1^2e_2 \\ \quad + e_2x_*^2 + e_1^2y_* + x_*^2y_* + 2e_1e_2x_* + 2e_1x_*y_*, \end{array} \right. \quad (3.6)$$

where $\kappa_1 > 0$ and $\kappa_2 > 0$ are control gains. Furthermore, substituting the control inputs Eq (3.6) into Eqs (3.2) and (3.5), we get the modified error dynamical system

$$\left\{ \begin{array}{l} \frac{de_1}{dt} = -(\kappa_1 + a)e_1 - e_b e_2 - e_b y_*, \\ \frac{de_2}{dt} = -\kappa_2 e_2 - e_c - e_b e_2 - e_b y_* \end{array} \right. \quad (3.7)$$

and

$$\left\{ \begin{array}{l} \frac{dv_I}{dt} = -(\kappa_1 + a)e_1^2 - \kappa_2 e_2^2 - e_c(e_2 + \frac{dc}{dt}) \\ \quad - e_b(e_1e_2 + e_1y_* + e_2^2 + y_*e_2 + \frac{db}{dt}) < 0. \end{array} \right. \quad (3.8)$$

Equation (3.8) is negative definite, which shows that the error dynamical system (3.2) tends to zero using the control inputs (3.6), resulting in $x \rightarrow x_1$, $y \rightarrow y_1$ as $t \rightarrow \infty$. Controller (3.6) depends on anonymous parameters. Thus, according to Eq (3.8), the updated law becomes

$$\left\{ \begin{array}{l} \frac{db}{dt} = \kappa_3 e_b - e_1e_2 - e_1y_* - e_2^2 - y_*e_2, \\ \frac{dc}{dt} = \kappa_4 e_c - e_2, \end{array} \right. \quad (3.9)$$

where κ_3 and κ_4 are greater than zero.

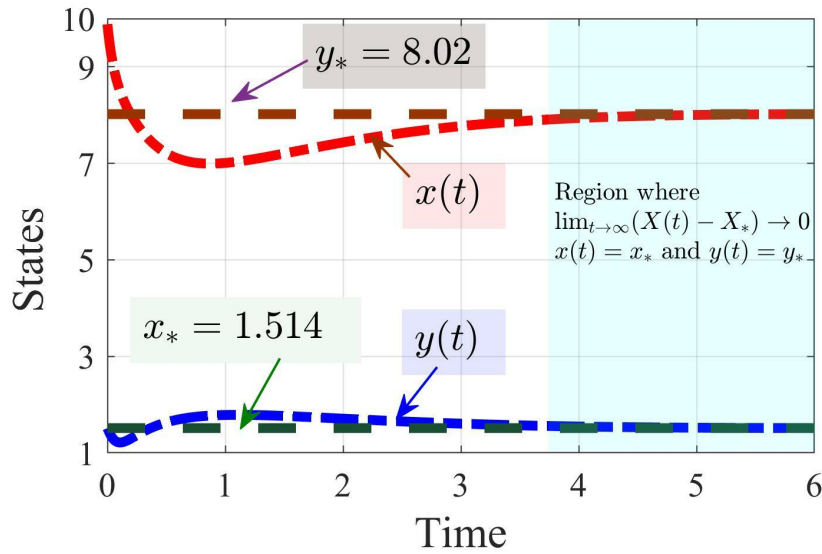


Figure 5. State variables $x(t)$, $y(t)$ approaching its desired values as time tends to infinity.

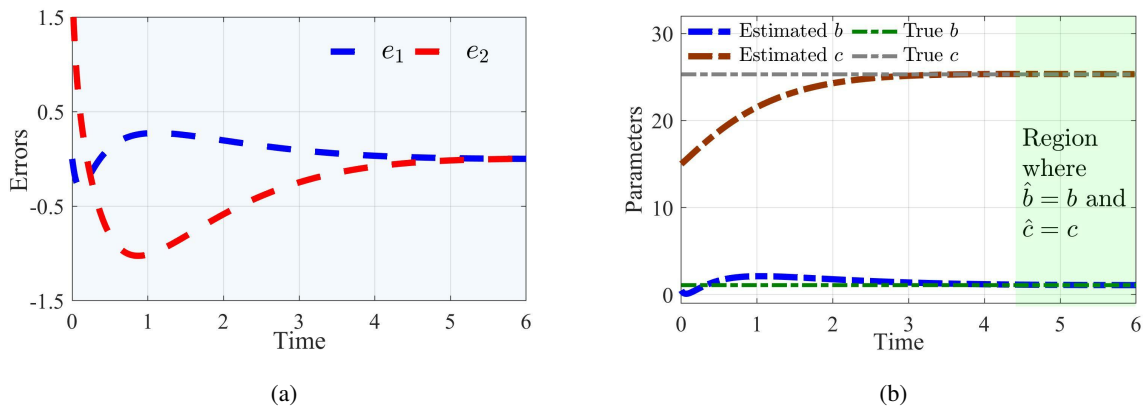


Figure 6. (a) Error terms approach zero, and (b) shows the unknown parameters \hat{b} and \hat{c} approaching their original parameters b and c , respectively, when time tends to infinity.

Figures 5 and 6 are the qualitative analysis and validation of analytical results given in Eqs (3.1)–(3.9). In Figure 5, the state variables $x(t)$ and $y(t)$ are shown approaching their desired values ($x_* = 1.514$, $y_* = 8.02$). Moreover, in Figure 5, the green and brown colored lines show the desired values, selected as stable reference points, to confirm that the original state variables, i.e., $x(t)$ (blue) and $y(t)$ (red) of system (3.1), approach stable equilibria as time ($t \rightarrow \infty$). Figure 6(a) confirms the analytical result of error dynamical system (3.7) with $\kappa_1 \geq 10$ and $\kappa_2 \geq 10$ in the presence of update law (3.9) shown in Figure 6(b), where the estimated parameters, i.e., \hat{b} and \hat{c} approach their original parameter values at time ($t \approx 4$).

From a chemical reaction perspective, control inputs $\rho_1(t)$ and $\rho_2(t)$ act as the external actuators to interpret the external flow of species D_1 and D_2 , respectively, and force the system to converge

toward the desired states with the aid of error terms, deviating from the desired concentrations of D_1 and D_2 . As the estimated parameters are unknown due to uncertain reaction rates, the controlled system continuously estimates them. However, system (1.2) measures the concentrations of both species, D_1 and D_2 , and adjust the estimate of original parameters to match the observed dynamics.

4. Conclusions

A dynamical model based on two-species chemical reactions has been considered in this paper. Researchers have analyzed codimension-one bifurcations and limit cycles for this model, but we have discussed higher codimension bifurcations and their physical implementation to demonstrate their role in enhancing system dynamics. The bifurcation parameters b and c have been treated as unknown, and a control strategy using parameter identification and Lyapunov theory has been employed to regulate oscillations. First, a Hessian matrix-based technique has been used to ensure the existence of codimension-two BT bifurcation and has provided unfolding parameters for studying local bifurcation curves. These trajectories have been plotted in Figure 2 and discussed mathematically. Further analysis of the BT bifurcation has revealed that codimension-three bifurcation occurs when the non-degeneracy condition $a_2b_2 = 0$ holds. Among available computational methods, a seven-step approach has been used to derive the normal form and compute the unfolding parameters ξ_1 , ξ_2 , and ξ_3 . Second, a positive definite function from Lyapunov theory has been applied to unknown and estimated bifurcation parameters to control solution randomness. The analytical results have been linked to physical interpretations through qualitative analysis, highlighting their impact on the system for reader clarity.

Use of AI tools declaration

No artificial intelligence tools were used in the preparation of this manuscript.

Acknowledgments

This work was supported by the National Natural Science Foundation of China, Grant No. 12471166 (F. Li); the Natural Science Foundation of Shandong Province, China, Grant No. ZR2024MA037 (F. Li); Shandong Province Science and Technology-Based SMEs Enhancement Program Project No. 2024TSGC0814 (H.W. Li)

Conflict of interest

The authors declare that they have no known competing financial interests or personal relationships that could have appeared to influence the work reported in this paper.

Author contributions

Xue Zhang: Writing – review & editing, Software, Validation, Methodology, Investigation. Jinzhao Whang: Software, Validation, Formal analysis, Investigation. Feng Li: Writing – review & editing, Supervision, Funding acquisition. Hongwei Li: Conceptualization, Methodology, Writing – original

draft, Supervision, Project administration. Muhammad Marwan: Writing – original draft, Software, Methodology, Investigation, Formal analysis, Conceptualization.

References

1. Q. Din, T. Donchev, D. Kolev, Stability, bifurcation analysis and chaos control in chlorine dioxide–iodine–malonic acid reaction, *MATCH Commun. Math. Comput. Chem.*, **79** (2018), 577–606. Available from: https://match.pmf.kg.ac.rs/electronic_versions/Match79/n3/match79n3_577-606.pdf.
2. M. Chen, X. Z. Li, Stability analysis and Turing pattern of an enzyme-catalyzed reaction model, *MATCH Commun. Math. Comput. Chem.*, **94** (2025), 195–206. <https://doi.org/10.46793/match.94-1.195C>
3. M. A. Khan, Q. Din, Codimension-one and codimension-two bifurcations of a fractional-order cubic autocatalator chemical reaction system, *MATCH Commun. Math. Comput. Chem.*, **91** (2024), 415–452. <https://doi.org/10.46793/match.91-2.415K>
4. H. Nabila, H. Tayebb, Nonlinear dynamics of fractional-order chaotic chemical reactor system based on the adomian decomposition method and its control via adaptive sliding mode control, *MATCH Commun. Math. Comput. Chem.*, **94** (2025), 355–378. <https://doi.org/10.46793/match.94-2.355N>
5. M. A. Khan, M. S. Khan, Q. Din, Codimension-one and codimension-two bifurcations of a modified Brusselator model, *Int. J. Dyn. Control*, **13** (2025), 154. <https://doi.org/10.1007/s40435-025-01652-3>
6. Y. Huang, X. S. Yang, Chaoticity of some chemical attractors: A computer assisted proof, *J. Math. Chem.*, **38** (2005), 107–117. <https://doi.org/10.1007/s10910-005-4537-2>
7. C. Xu, Y. Wu, Bifurcation and control of chaos in a chemical system, *Appl. Math. Model.*, **39** (2015), 2295–2310. <https://doi.org/10.1016/j.apm.2014.10.030>
8. R. Wu, L. Yang, Bogdanov-Takens bifurcation of an enzyme-catalyzed reaction model, *Nonlinear Dyn.*, **112** (2024), 14363–14377. <https://doi.org/10.1007/s11071-024-09868-2>
9. M. Izadi, H. Ahmad, H. M. Srivastava, Numerical computations of time-dependent auto-catalytic glycolysis chemical reaction-diffusion system, *MATCH Commun. Math. Comput. Chem.*, **93** (2025), 69–97. <https://doi.org/10.46793/match.93-1.069I>
10. Z. M. Alaof, K. K. Ali, M. S. Mehanna, A. H. Abdel-Aty, M. A. Shaalan, Applications of the Belousov–Zhabotinsky reaction–diffusion system: Analytical and numerical approaches, *Open Phys.*, **23** (2025), 20250129. <https://doi.org/10.1515/phys-2025-0129>
11. C. Zhou, F. Xie, Z. Li, Complex bursting patterns and fast-slow analysis in a smallest chemical reaction system with two slow parametric excitations, *Chaos Soliton Fractals*, **137** (2020), 109859. <https://doi.org/10.1016/j.chaos.2020.109859>
12. J. H. Merkin, A. F. Taylor, Reduction waves in the two-variable Oregonator model for the BZ reaction, *Physica D*, **241** (2012), 1336–1343. <https://doi.org/10.1016/j.physd.2012.04.007>
13. Q. Din, U. Saeed, Stability, discretization, and bifurcation analysis for a chemical reaction system, *MATCH Commun. Math. Comput. Chem.*, **90** (2023), 151–174. <https://doi.org/10.46793/match.90-1.151D>
14. D. Erle, Nonoscillation in closed reversible chemical systems, *J. Math. Chem.*, **27** (2000), 293–302. <https://doi.org/10.1023/A:1018871722219>

15. S. Azimi, C. Panchal, A. Mizera, I. Petre, Multi-stability, limit cycles, and period-doubling bifurcation with reaction systems, *Int. J. Found. Comput. Sci.*, **28** (2017), 1007–1020. <https://doi.org/10.1142/S0129054117500368>
16. B. Fercec, I. Nagy, V. G. Romanovski, G. Szederkényi, J. Tóth, Limit cycles in a two-species reaction, *J. Nonlinear Model. Anal.*, **1** (2019), 283–300. <https://doi.org/10.12150/jnma.2019.283>
17. I. Nagy, V. G. Romanovski, J. Tóth, Two nested limit cycles in two-species reactions, *Mathematics*, **8** (2020), 1658. <https://doi.org/10.3390/math8101658>
18. M. Banaji, B. Boros, The smallest bimolecular mass action reaction networks admitting Andronov–Hopf bifurcation, *Nonlinearity*, **36** (2023), 1398. <https://doi.org/10.1088/1361-6544/acb0a8>
19. M. Ch-Chaoui, K. Mokni, A discrete evolutionary Beverton–Holt population model, *Int. J. Dyn. Control*, **11** (2023), 1060–1075. <https://doi.org/10.1007/s40435-022-01035-y>
20. H. Mouhsine, H. Ben Ali, K. Mokni, M. Ch-Chaoui, Dynamics unveiled: Investigating bifurcations and the strong Allee effect in a discrete-time prey-predator system, *Int. J. Dyn. Control*, **13** (2025), 324. <https://doi.org/10.1007/s40435-025-01834-z>
21. M. Marwan, N. Wang, F. Li, Practical computation of higher codimension Bogdanov-Takens bifurcations in energy supply-demand system, *Math. Comput. Simul.*, **238** (2025), 255–268. <https://doi.org/10.1016/j.matcom.2025.05.004>
22. M. Marwan, M. Han, M. Osman, Hidden covers (wings) in the fractals of chaotic systems using advanced Julia function, *Fractals*, **31** (2023), 2350125. <https://doi.org/10.1142/S0218348X23501256>
23. Y. Xu, Y. Yang, F. Meng, S. Ruan, Degenerate codimension-2 cusp of limit cycles in a Holling-Tanner model with harvesting and anti-predator behavior, *Nonlinear Anal. Real World Appl.*, **76** (2024), 103995. <https://doi.org/10.1016/j.nonrwa.2023.103995>
24. X. Gao, Y. Jin, M. Marwan, F. Li, Y. Wei, Impact of Hopf and Bautin bifurcations on an autocatalytic chemical reaction system, *MATCH Commun. Math. Comput. Chem.*, **94** (2025), 863–889. <https://doi.org/10.46793/match94-3.09225>
25. Y. A. Kuznetsov, Practical computation of normal forms on center manifolds at degenerate Bogdanov-Takens bifurcations, *Int. J. Bifurcation Chaos*, **15** (2005), 3535–3546. <https://doi.org/10.1142/S0218127405014209>
26. F. A. Carrillo, F. Verduzco, J. Delgado, Analysis of the Takens-Bogdanov bifurcation on m -parameterized vector fields, *Int. J. Bifurcation Chaos*, **20** (2010), 995–1005. <https://doi.org/10.1142/S0218127410026277>
27. X. Liu, S. Liu, Codimension-two bifurcation analysis in two-dimensional Hindmarsh-Rose model, *Nonlinear Dyn.*, **67** (2012), 847–857. <https://doi.org/10.1007/s11071-011-0030-6>
28. G. Peng, Y. Jiang, Practical computation of normal forms of the Bogdanov-Takens bifurcation, *Nonlinear Dyn.*, **66** (2011), 99–132. <https://doi.org/10.1007/s11071-010-9914-0>
29. C. Li, J. Li, Z. Ma, Codimension 3 B-T bifurcations in an epidemic model with a nonlinear incidence, *Discrete Contin. Dyn. Syst. Ser. B*, **20** (2015), 1107–1116. <https://doi.org/10.3934/dcdsb.2015.20.1107>

30. B. Zeng, P. Yu, M. Han, An efficient solution procedure for solving higher-codimension Hopf and Bogdanov-Takens bifurcations, *Commun. Nonlinear Sci. Numer. Simul.*, **138** (2024), 108241. <https://doi.org/10.1016/j.cnsns.2024.108241>
31. F. Takens, Forced oscillations and bifurcations, in *Global analysis of dynamical systems*, Institute of Physics (IOP) Publishing, (2001), 1–61. Available from: <https://zbmath.org/1702959>.
32. R. I. Bogdanov, Bifurcation of the limit cycle of a family of plane vector fields, *Sel. Math. Sov.*, **1** (1981), 373–387. Available from: <https://istina.msu.ru/publications/article/2336810/>.
33. Z. Liu, P. Magal, D. Xiao, Bogdanov-Takens bifurcation in a predator-prey model, *Z. Angew. Math. Phys.*, **67** (2016), 137. <https://doi.org/10.1007/s00033-016-0724-1>
34. M. Lu, C. Xiang, J. Huang, Bogdanov-Takens bifurcation in a SIRS epidemic model with a generalized non-monotone incidence rate, *Discrete Contin. Dyn. Syst. Ser. S*, **13** (2020), 3125–3138. <https://doi.org/10.3934/dcdss.2020115>
35. S. Wang, H. Yu, Equilibria and Bogdanov-Takens bifurcation analysis in the Bazykin's predator-prey system, *Discrete Dyn. Nat. Soc.*, **2022** (2022), 4844228. <https://doi.org/10.1155/2022/4844228>
36. I. Al-Darabsah, S. A. Campbell, M-current induced Bogdanov-Takens bifurcation and switching of neuron excitability class, *J. Math. Neurosci.*, **11** (2021), 1–26. <https://doi.org/10.1186/s13408-021-00103-5>
37. F. Li, M. Marwan, K. Karawanich, On the bifurcations in a quadrotor unmanned aerial vehicle dynamical system using normal form theory, *Nonlinear Dyn.*, **113** (2025), 6405–6425. <https://doi.org/10.1007/s11071-024-10483-4>
38. M. Marwan, M. Z. Abidin, On the analytical approach of codimension-three degenerate Bogdanov-Takens (B-T) bifurcation in satellite dynamical system, *J. Nonlinear Model. Anal.*, **5** (2023), 667–681. <https://doi.org/10.12150/jnma.2023.667>
39. L. Fortuna, M. Frasca, A. Buscarino, *Optimal and Robust Control: Advanced Topics with MATLAB®*, CRC Press, 2021. <https://doi.org/10.1201/9781003196921>
40. F. Lin, G. Xue, B. Qin, S. Li, H. Liu, Event-triggered finite-time fuzzy control approach for fractional-order nonlinear chaotic systems with input delay, *Chaos Solitons Fractals*, **175** (2023), 114036. <https://doi.org/10.1016/j.chaos.2023.114036>
41. X. Li, S. Lu, Z. Yu, S. Wu, F. Yang, Hybrid control strategy and optimal control for rumor spreading, *Chaos Solitons Fractals*, **195** (2025), 116180. <https://doi.org/10.1016/j.chaos.2025.116180>
42. J. Iqbal, S. Ahmad, M. Marwan, A. Rafiq, Control analysis of virotherapy chaotic system, *J. Biol. Dyn.*, **16** (2022), 585–595. <https://doi.org/10.1080/17513758.2022.2104391>
43. M. Marwan, S. Ahmad, M. Aqeel, M. Sabir, Control analysis of Ruckledge chaotic system, *J. Dyn. Syst. Meas. Control*, **141** (2019), 041010. <https://doi.org/10.1115/1.4042030>
44. M. Ch-Chaoui, K. Mokni, A multi-parameter bifurcation analysis of a prey–predator model incorporating the prey Allee effect and predator-induced fear, *Nonlinear Dyn.*, **113** (2025), 18879–18911. <https://doi.org/10.1007/s11071-025-11063-w>

Appendix A

The following analytical formulas given in [26] are used to compute the parameter values to check the existence of codim-2 BT bifurcation

$$\begin{aligned}\bar{a} &\equiv \frac{1}{2} p_1^T (q_2 \bullet D^2 F(X_0, \mu_0)) p_1, \\ \bar{b} &\equiv p_1^T (q_1 \bullet D^2 F(X_0, \mu_0)) p_1 + p_1^T (q_2 \bullet D^2 F(X_0, \mu_0)) p_2.\end{aligned}$$

If $\bar{a}\bar{b} \neq 0$, then S_1 and S_2 are used to find the unfolding parameters

$$\begin{aligned}S_1^T &\equiv q_2^T F_\mu(X_0, \mu_0), \\ S_2 &\equiv \left[\frac{2\bar{a}}{\bar{b}} (p_1^T (q_1 \bullet D^2 F(X_0, \mu_0)) p_2 + p_2^T (q_2 \bullet D^2 F(X_0, \mu_0)) p_2) - p_1^T (q_2 \bullet D^2 F(X_0, \mu_0)) p_2 \right] \\ &\quad \times F_\mu^T(X_0, \mu_0) q_1 - \frac{2\bar{a}}{\bar{b}} \sum_{i=1}^2 (q_i \bullet F_{\mu X}(X_0, \mu_0)) p_i + (q_2 \bullet F_{\mu X}(X_0, \mu_0)) p_1,\end{aligned}$$

where p_0, p_1 are the left and q_0, q_1 are right generalized eigenvectors. Furthermore, if $\bar{a}\bar{b} = 0$, then the analytical formulas given in this Appendix are invalid to use and indicate the possibility of codim-3 BT bifurcation.



AIMS Press

©2026 the Author(s), licensee AIMS Press. This is an open access article distributed under the terms of the Creative Commons Attribution License (<https://creativecommons.org/licenses/by/4.0>)